Nat. Hazards Earth Syst. Sci., 11, 3275–3291, 2011
www.nat-hazards-earth-syst-sci.net/11/3275/2011/
doi:10.5194/nhess-11-3275-2011


Natural Hazards and Earth System Sciences

# Impacts of projected maximum temperature extremes for C21 by an ensemble of regional climate models on cereal cropping systems in the Iberian Peninsula

**M. Ruiz-Ramos**[1], **E. Sánchez**[2], **C. Gallardo**[3], **and M. I. Mínguez**[1]

[1]AgSystems Group, Universidad Politécnica de Madrid, ETSI Agrónomos, 28040 Madrid, Spain
[2]Facultad de Ciencias del Medio Ambiente, Univ. Castilla-La Mancha, Avda. Carlos III s/n, 45071 Toledo, Spain
[3]Instituto de Ciencias Ambientales, Univ. Castilla-La Mancha, Avda. Carlos III s/n, 45071 Toledo, Spain

Received: 14 February 2011 – Revised: 5 July 2011 – Accepted: 19 October 2011 – Published: 12 December 2011

**Abstract.** Crops growing in the Iberian Peninsula may be subjected to damagingly high temperatures during the sensitive development periods of flowering and grain filling. Such episodes are considered important hazards and farmers may take insurance to offset their impact. Increases in value and frequency of maximum temperature have been observed in the Iberian Peninsula during the 20th century, and studies on climate change indicate the possibility of further increase by the end of the 21st century. Here, impacts of current and future high temperatures on cereal cropping systems of the Iberian Peninsula are evaluated, focusing on vulnerable development periods of winter and summer crops. Climate change scenarios obtained from an ensemble of ten Regional Climate Models (multimodel ensemble) combined with crop simulation models were used for this purpose and related uncertainty was estimated. Results reveal that higher extremes of maximum temperature represent a threat to summer-grown but not to winter-grown crops in the Iberian Peninsula. The study highlights the different vulnerability of crops in the two growing seasons and the need to account for changes in extreme temperatures in developing adaptations in cereal cropping systems. Finally, this work contributes to clarifying the causes of high-uncertainty impact projections from previous studies.

## 1 Introduction

Crop growth and development rates are closely linked to temperature. In both cases, the responses are non-linear, increasing from zero at a lower threshold temperature to an optimum temperature range and then decreasing, ultimately again to zero, at a higher threshold; these are the cardinal temperatures. Crops accumulate less biomass and develop more slowly outside the optimum range and are vulnerable to damage and death at high and low extremes (Coehlo and Dale, 1980; Porter and Gawith, 1999), with different susceptibilities during individual stages of development, e.g. flowering and grain set as opposed to vegetative growth (e.g. for cereals see Al-Khartib and Paulsen, 1984). Extreme high temperatures may damage or kill plants at susceptible phases, or decrease crop yield (see Wheeler et al., 2000 for quantification of decrease in crop yields and yield components) even if plants survive. Differences of adaptation of individual species to climatic conditions are largely determined by these daily temperature responses (Gilmore and Rogers, 1958 for maize). These responses are included in crop simulation models, often constructed as piece-wise linear functions around four cardinal temperatures for individual species. Crop simulation models estimate duration of development phases (phenophases) with "thermal time", which is the accumulated exposure to average daily temperature above a threshold or base temperature (an integral of degree days, °C d) specific to each species or cultivar under which there is no development progression. The duration of some phases are also affected by the day length (Loomis and Connor, 1996). Phenophase duration (e.g. days from emergence to flowering or grain filling duration) is correlated to average temperature.

The Iberian Peninsula (IP) presents aspects of specific interest within European climate. Current maximum temperatures ($T_{\max}$) above damage threshold are extreme events with important agricultural impact if appearing during sensitive crop phenophases. In the last decades, an increase in $T_{\max}$ values has been observed in the IP (del Río et al., 2007), as well as in extreme $T_{\max}$ events (Hertig et al., 2010). In



*Correspondence to:* M. Ruiz-Ramos
(margarita.ruiz.ramos@upm.es)

Europe, an example of damages was the heat wave of 2003 (Schär et al., 2004) that caused a reduction in primary productivity, including crop yields (Ciais et al., 2005).

In the Fourth Assessment Report of the Intergovernmental Panel on Climate Change (IPCC), the IP is referred to as being significantly affected by climate change because projections of increase in mean temperature, $T_{max}$, water stress, and extreme events are among the largest in Europe (Alcamo et al., 2007; Christensen et al., 2007). Ecophysiological crop simulation models are the main integrating tool to evaluate impact of future conditions and extreme events on agricultural productivity. The climatic data needed as inputs in crop simulation models are provided by global climate models (GCMs). These models generate the variables simulating present and future climate, the latter under different scenarios of greenhouse gas emissions, but at a spatial resolution that is usually too poor for impact studies. Several methodologies have been proposed for increasing the spatial details of GCMs outputs, and Regional Climate Models (RCMs) have been one of the most successful and used (Giorgi et al., 2001). RCMs are models conceptually similar to GCMs, but are applied to a limited region of the planet, thus needing inputs from GCMs for atmospheric variables as the lateral boundary conditions of the domain or region where they are being applied. Additionally, RCMs have a greater grid resolution. This methodology gives better results in complex orographic regions, heterogeneous land-surface conditions and terrains and coastal processes (Mearns et al., 2003) as with the IP (Guereña et al., 2001), enabling regional impact studies. Extreme event studies also benefit from the high resolution of RCM in comparison to GCMs (Beniston et al., 2007).

Studies on regional climate change with RCMs over Europe project an increase in average, minimum, and maximum temperatures (Christensen et al., 2007; Déqué et al., 2007), as well as in events of extreme $T_{max}$ either in frequency or in intensity (Beniston et al., 2007, Kjellström et al., 2007, Diffenbaugh et al., 2007 and Sánchez et al., 2004 for the Mediterrenean area including the IP). The impacts on crops are the result of the interaction of these projected increases with other effects that climate change may have on crops, mainly due to $CO_2$ increased concentration (Ainsworth et al., 2009), and on crop phenology (Guereña et al., 2001; Rosenzweig et al., 2000; Sadras and Monzon, 2006). Thus, climate change alters timing and duration of vulnerable phenological phases. Projections of extreme events during these vulnerable periods are referred to here as "effective impact".

The use of an ensemble of climate models that have different parameterizations and numerical schemes to simulate the atmospheric processes generates a range of possible results that enable the evaluation of uncertainties. Uncertainties of impact projections should also be estimated, as with climate projections (Déqué et al., 2007), because they are incorporated along the modelling climate-to-impact chain. Uncertainties linked to crop simulation models have to be added to the former (Ruiz-Ramos and Mínguez, 2010). Modelling chains, with or without the use of ensembles, are currently a standard methodology in this type of studies (Alcamo et al., 2007; and specifically for the Iberian Peninsula, Mínguez et al., 2007; Ruiz-Ramos and Mínguez, 2010). This approach has also been used for impact of extreme events on crops under climate change conditions, either using GCMs or RCMs. For example, Rosenzweig et al. (2000) have analysed expected impacts of average temperature increase in the USA, including extreme events of $T_{max}$, finding a probable reduction on potential crop yield and severe economic losses due to "extremely high temperatures" in the 2030s. In northern Europe, Semenov (2009) has studied changes in the probability of heat stress around flowering of wheat for the 2020s and the 2050s, using a wheat simulation model combined with high-resolution climate scenarios based on the output from a RCM, while Semenov and Stratonovich (2010) studied the same variable in northern, central and southern Europe for the 2046–2065 period. In the Mediterranean area, Alcamo et al. (2007) report increases in the frequency of extreme climate events such as heat stress during flowering period by the end of the C21. Also in the Mediterranean and for the last decades of C21, these increases have been projected by Moriondo et al. (2010a) using data from a RCM. Moriondo and Bindi (2006) have studied the frequency of events with $T_{max}$ above and stressful thresholds for a summer and a winter crop, comparing results when applying outputs from a GCM, a RCM, and statistical downscaling to a crop model. Studies with RCM ensembles are few (of the ones cited above, only that of Semenov and Startonovich (2010) uses an ensemble of GCMs in combination with a weather generator), so the evaluation of uncertainties associated to projections is difficult. Furthermore, studies covering climate variability at site level are also scarce; Semenov and Stratonovich (2010) include one Spanish site, and Moriondo et al. (2010a) support the capability of the crop model on comparison to EUROSTAT database.

Our former work and in particular Ruiz-Ramos and Mínguez (2010) were focused on means, interannual variability and their related uncertainty, and did not include any extreme analysis. Extremes do not present the same statistical nor climatic behaviour as means and their estimation usually shows greater uncertainty than mean trends. Their effect on crops can be also very different and relevant for risk management and insurance companies. For this reason, the present work is devoted specifically to extreme events relevant for the IP. The objective of this paper is to generate projections of changes in the effective impact of $T_{max}$ extreme events in winter and summer crops under climate change scenarios. Projections are done for 11 representative locations of the IP with a multimodel ensemble of RCMs in combination with crop simulation models, i.e. a climate-impact ensemble, to evaluate uncertainties associated to these projections with the aim of improving future adaptation strategies of cropping systems.

The paper has been organized as follows: the methodology section presents the climate data used, the crop modelling guidelines, the extremes indices selected, and the uncertainty treatment. The results section begins with the results for climatic-only indices, followed by the results from stress indices due to $T_{\max}$ extremes events. Summer and winter crops have been analized separately and uncertatinty is included for both of them. The paper ends with a general discussion and the main conclusions of this study.

## 2 Material and methods

### 2.1 Ensemble of climate models

The regional climate multimodel ensemble generated by the European Project PRUDENCE (ref. EVK2-2001-00156, Christensen and Christensen, 2007) was used in this work with the following 10 RCMs: HIRHAM (DMI), ARPEGE (CNRM), HadRM3H (HC), CHRM (ETH), CLM (GKSS), REMO (MPI), RCAO (SMHI), PROMES (UCLM), RegCM (ICTP) and RACMO (KNMI). The RCMs were nested in the GCM HadAM3H and two RCMs, ARPEGE and RCAO, used the boundary conditions of the GCMs HadCM3 and ECHAM/OPYC4, respectively. Simulations were used for the 1961–1990 period and scenario SRES A2 of IPCC (635–856 ppm $CO_2$, Nakicenovic and Swart, 2000) for the 2070–2100 period, at a horizontal resolution of 50 km × 50 km. The variables taken from the RCMs used are daily $T_{\max}$ and $T_{\min}$, incident solar radiation, relative humidity and wind speed. The biases of RCMs with regard to present climate are analysed in Jacob et al. (2007), showing that biases over the IP are small compared to other European regions.

### 2.2 Crop modelling

A climate-impact modelling chain is established when daily outputs from the ensemble of climate models are used as inputs in the crop simulation models, and an ensemble of crop yield projections is built (climate-impact ensemble). The crop models used were CERES-maize (Ritchie and Otter, 1985) and CERES-wheat (Jones and Kiniry, 1986) from DSSAT platform (Tsuji et al., 1994). These crop models simulate crop physiological processes, water and nitrogen balances, include species and cultivar characteristics, and their management using as inputs climate variables and soil parameters. Main outputs are biomass, yield, water use, and phenology (phenostages and phenophases). Each cultivar has specific needs of thermal time to complete each phenophase, and also optimum, sub-optimum and threshold damage temperatures. Crop development cycle (from sowing and emergence, to physiological maturity) progresses by daily thermal or photo-thermal accumulation: it is computed as the sum of degree-days or degree-hours-days. The crop models used in this study have been previously calibrated and validated for various Iberian locations and crops (for southern locations: Mariscal, 1993; Rebollo, 1993; for southwest, northeast, northern, southern and centre Plateaux: Iglesias and Mínguez, 1995; for northwest: López-Cedrón et al., 2005; for wheat and maize applicable to all IP: Quemada et al., 1997). Methodology and most yield projections have been described in Mínguez et al. (2004, 2007) and Ruiz-Ramos and Mínguez (2010).

The crops chosen were maize and wheat because they represent summer and winter season crops, respectively. Moreover, these crops have different temperature responses: wheat is mostly adapted to temperate regions and has a "C3 photosynthetic pathway" for $CO_2$ fixation; and maize is a "C4" species, adapted to warmer climates, and thus grown in summer in temperate regions as it is damaged by temperatures below 8–10 °C (Gardner et al., 1985). Both crops were simulated with irrigation (water non-limiting and maximum crop evapotranspiration) to eliminate the effect of changes in precipitation and focus on $T_{\max}$ effects. A "spring wheat" cultivar was chosen to eliminate vernalisation requirement for flowering ("winter wheat" require exposure to low temperatures, $0\,^{\circ}\mathrm{C} > T > 6–7\,^{\circ}\mathrm{C}$, to induce flowering).

Sowing dates for maize were all in spring, ranging from 30 March in the South of the Iberian Peninsula, 16 April in the Centre, and 16 May in the North; this delay is needed to avoid frost and low temperatures. Wheat was sown in autumn (10 November) for all locations. The outputs from the models used here were dates of emergence (plant appearance above the soil after sowing), flowering, and physiological maturity of the crops, simulated for 11 representative locations of main agricultural areas (Fig. 1).

### 2.3 Extreme $T_{\max}$ indices

Indices were established for flowering and grain filling of wheat and maize and were based on temperature thresholds. $T_{\max}$ damage threshold for flowering of wheat was set at 31 °C, and for grain filling at 35 °C, based on averaged values from the literature recompiled by Porter and Gawith (1999). For maize, the threshold chosen for both stages was 35 °C, as used by Mearns et al. (1984). Two types of extreme events were used as in Mearns et al. (1984), summarised in Table 1: (1) 31-1d or 35-1d: number of days with $T_{\max}$ above thresholds 31 °C and 35 °C, respectively, and (2) 31-5d or 35-5d: number of events with at least 5 consecutive days with temperatures above 31 °C and 35 °C, respectively.

Extreme events are usually considered in a specific period, e.g. a month (Mearns et al. (1984) have calculated these events for July in the case of maize). In our work we link the occurrence of extreme events to the development of the crop. To achieve this we have established 3 periods for wheat and maize: (1) YEAR: evaluation of the 12 months or annual impact; (2) FLO: anthesis or flowering, with a fixed duration of 30 days starting 15 days before flowering date and ending 15 days after, i.e. this is a mobile period; and

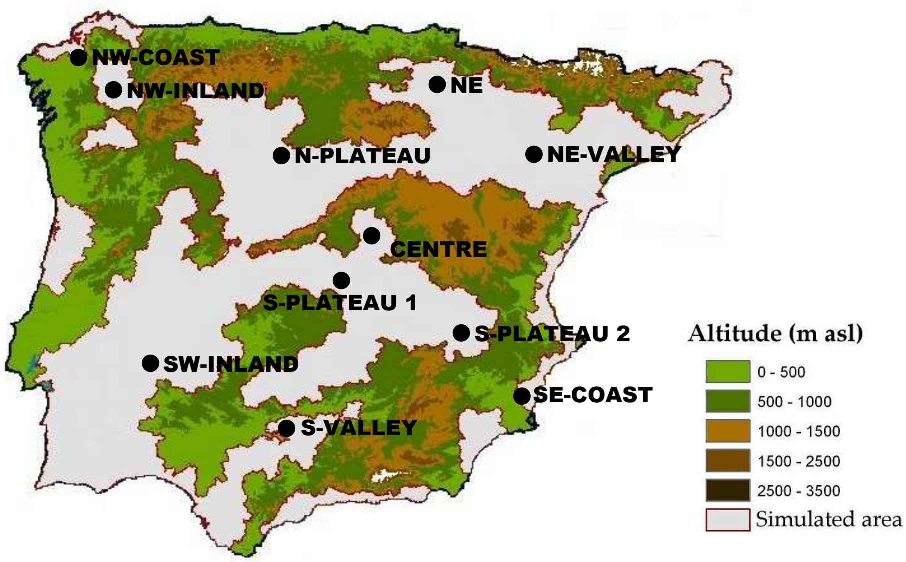


**Fig. 1.** Locations chosen from representative agricultural regions in the Iberian Peninsula that differ in climate, growing conditions and cropping systems. Altitude of NW- and SE-Coast regions is below 50 m above sea level (a.s.l.); SW-Inland, NE-Valley and S-Valley is between 100 and 250 m a.s.l.; NW-Inland and NE are between 450 and 500 m a.s.l. and close to mountain areas; N Plateau, Centre and S-Plateau 1 and 2 are between 550 and 700 m a.s.l.

**Table 1.** Indices calculated for maize and wheat, specifying temperature threshold and period: for climatic indices, period YEAR (annual), and for stress indices, periods FLO (from 15 days before flowering to 15 days after flowering) and GRAIN (from 15 days before flowering to physiological maturity).

| | MAIZE | WHEAT | |
|---|---|---|---|
| | THRESHOLD 35 °C | THRESHOLD 35 °C | THRESHOLD 31 °C |
| Climatic indices | | | |
| YEAR* | 35-1d, 35-5d | 35-1d, 35-5d | 31-1d, 31-5d |
| Stressindices | | | |
| FLO | 35-1d, 35-5d | – | 31-1d, 31-5d |
| GRAIN | 35-1d, 35-5d | 35-1d, 35-5d | – |

*For maize: from 1 January to 31 December; for wheat: from 1 October to 30 September

(3) GRAIN: flowering to maturity with variable duration, starting 15 days before flowering and ending in physiological maturity, hereafter referred to as grain filling. The 12-month period was established from 1 January to 31 December for maize (maize-YEAR), and from 1 October to 30 September for wheat (wheat-YEAR), in order to include whole crop cycle. Flowering and maturity dates were simulated for the 11 locations with the climate-impact ensemble. Ten different projections of phenological dates were obtained from each location by the climate-impact ensemble: one for each of the 10 RCM-crop model combination or ensemble member, each projection formed by a 30-yr simulation of current climate and a 30-yr simulation in future scenario conditions. Indices were obtained for 1-day and 5-day events for two crops, and for the 3 periods considered (YEAR, FLO and GRAIN); i.e. 6 indices of extreme events per crop (Table 1).

YEAR indices were called climatic indices because only the ensemble of climate models was used for its calculation (Déqué et al., 2007; Sánchez et al., 2004). FLO and GRAIN were climatic-phenological or stress indices that express effective impact and their calculation is linked to the vulnerable phenostage (flowering) or phenophase (grain filling) of the crop and were obtained with the climate-impact ensemble. In addition, the ratios GRAIN/YEAR and FLO/YEAR were calculated for each index, i.e. the fraction of the annual event YEAR that is damaging occurring during vulnerable periods of the phenostage FLO and phenophase GRAIN. These ratios express in percentage the relative frequency of stress in crop development in comparison with the annual impact, YEAR.

### 2.4 Uncertainty evaluation

Uncertainties associated to the indices were estimated by calculating the degree of coincidence between members of the climate-impact ensemble, as described in Ruiz-Ramos and Mínguez (2010). Briefly, the degree of coincidence was measured by comparing climatology (30-yr time series) from each RCM-crop model simulation of the same period, location and crop. SPSS software and Games-Howell test were used since the hypothesis of variance homogeneity was not always fulfilled (Field, 2005). The test established the percentage of matching pairs of time series that did not show significant difference; the larger the number of matching pairs, the lower the uncertainty.

## 3 Results and discussion

### 3.1 Climatic indices

In current climate, climatic indices for $T_{\text{max}}$ above 35 °C describe adequately the incidence of these extreme events in agreement with observed trends in frequency and intensity of those extreme events in the IP (del Río et al., 2007; Hertig et al., 2010). Projections in A2 scenario (2070–2100) show a significant increase in $T_{\text{max}}>35$ °C events (Figs. 2 and 3); these findings are also coherent with results in climate change by Beniston et al. (2007) and Kellsjtrom et al. (2007) where a significant increase of extreme events was obtained.

In particular, 35-1d-YEAR indices for maize-YEAR, beginning in January (Fig. 2), and for wheat-YEAR, beginning in October (Fig. 3), increase in A2 scenario, with a gradient of increase from north to south (Fig. 2). For both 1d and 5d event types, and both 31 °C and 35 °C thresholds, the indices differentiate two areas, the northwest (NW-INLAND and NW-COAST) with a smaller absolute increase in their values, and the rest of the IP. The difference between 5d and 1d events becomes larger in southern areas (Figs. 2, 3 and 4).

Mean coincidence between time series of ensemble members ranges from 45 % for maize (Table 2, YEAR indices) to 51 % for wheat (Table 3a, b, YEAR indices) in current climate for 1d indices, indicating a large uncertainty that decreased for A2 projections. For 5d indices, the uncertainty is smaller and mean coincidence of time series is above 70 % in current climate and ca. 80 % in A2 conditions; this indicates a robust result. The small uncertainty found describing the strongest events (i.e. 5d indices) as well as the observations carried out in the IP mentioned above confirm that using regional climate models is a suitable methodology for regional assessment. Moreover, it supports that studies dealing with extreme events relevant to impact and consistency with observations are improved by the high spatial resolution obtained by RCMs.

### 3.2 Stress indices (FLO and GRAIN): effective impact

#### 3.2.1 Summer crop: maize

Stress indices of $T_{\text{max}}$ that express effective impact in vulnerable periods in maize differ from climatic indices. In the case of grain filling period, 35-1d index increases in A2 scenario (2070–2100) more than the 35-5d index; the same areas as those found for climatic indices are differentiated, one in the northwest (NW-COAST and NW-INLAND) and the other including the rest of locations (Fig. 5). This spatial difference is also found during the period where flowering takes place (Fig. 6). During this phenostage, SE-COAST location behaves as locations in the north. Comparing the increase in A2 of climatic indices with that of stress indices, effective impact is found concentrated during grain filling and in 35-1d type events in the southern two-thirds of the IP.

Uncertainty in the estimation of stress indices is smaller than for climatic ones (Table 2). Uncertainty for GRAIN and FLO periods is overall smaller for A2 than for current climate, except in the north (NW-COAST, NW-INLAND, NE); for instance, under A2 conditions, the average coincidence found among ensemble members is above 70 % for 35-1d for both phenological periods, although uncertainty is larger during grain filling than during flowering. Locations on the coast (NW-COAST and SE-COAST) present smallest uncertainties (Table 2), which contrasts with the largest uncertainties found for these locations in previous work on yield impacts (Ruiz-Ramos and Mínguez, 2010). This may be due to the small number of these extreme events in coastal areas compared with inland locations of the same latitude (Figs. 2, 5 and 6). We can thus exclude $T_{\text{max}}$ as source of the large uncertainty found in these locations, due to the existing relationship between $T_{\text{max}}$ and extreme events reported by Mearns et al. (1984) and del Río et al. (2007).

GRAIN/YEAR and FLO/YEAR ratios indicate what part of the effective impact is concentrated in the vulnerable periods measured as the percentage represented by stress indices with respect to the annual climatic indices (Table 4); these ratios are in general largest in both Plateaux. Fifty-five to 90 % of 1d-type events take place during grain filling in current climate, and are reduced mainly in the centre and south Plateaux in A2. On the contrary, locations in the north (NW-COAST, NW-INLAND and NE) show an increase in the ratios. One-day events during flowering represent between 10 to 60 % of total annual events, decreasing in ca. 10 % in A2. Ratios for 5d-type events are smaller, and the main difference with 1d events is that the proportion of events during flowering increases in A2 in the northwest and south. Smallest values of the ratios are found in coastal locations (Table 4).

A smaller number of events are found in the two northern thirds of the IP, although effective impacts represent the largest proportion (>60 % during grain filling in A2) and uncertainties in projections are also larger. Several issues should be taken into account in order to explain the greater ratios in northern parts: (1) the cultivar and sowing dates

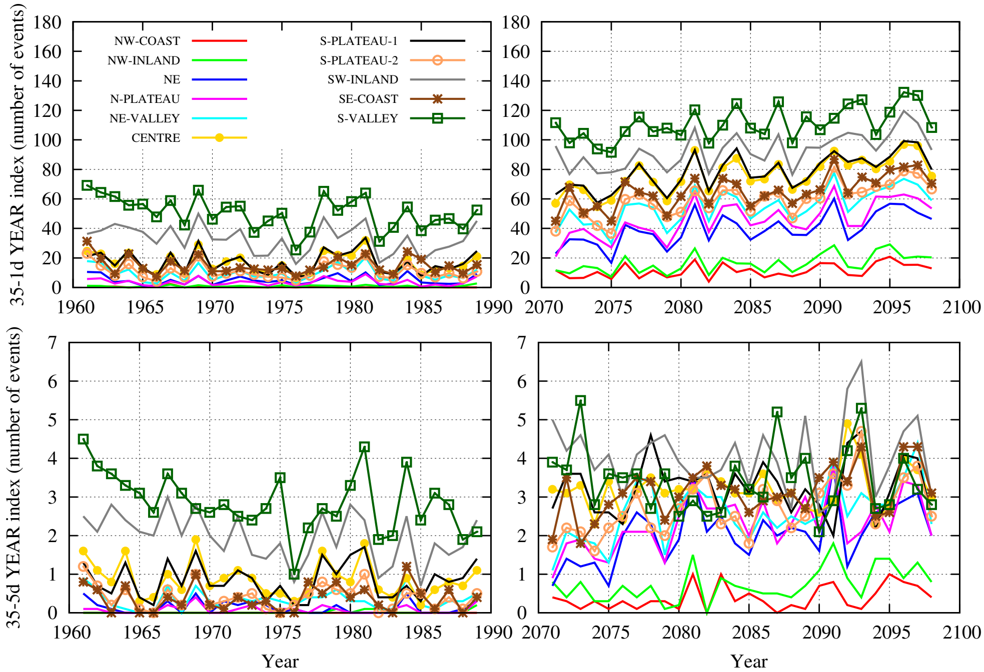


**Fig. 2.** Time series of extreme $T_{max}$ climatic indices (YEAR, annual impact from January to December) for maize at locations of Fig. 1. Left column shows results for the current climate and right column for the future scenario A2. Upper plots show the number of events with 1 day over the threshold of 35 °C (35-1d), and below, the number of events with 5 consecutive days over 35 °C (35-5d) are shown. Values correspond to the ensemble mean.

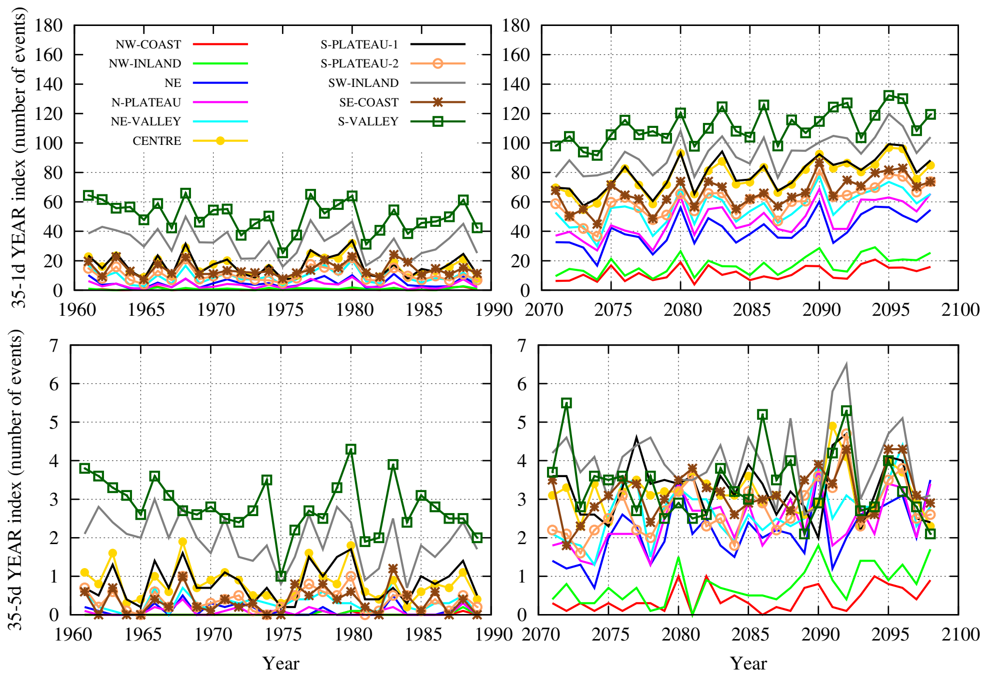


**Fig. 3.** Time series of extreme $T_{max}$ climatic indices (YEAR, annual impact from October to September) for irrigated spring wheat at locations of Fig. 1. Left column shows results for the current climate and right column for the future scenario A2. Upper plots show the number of events with 1 day over the threshold of 35 °C (35-1d), and below, the number of events with 5 consecutive days over 35 °C (35-5d) are shown. Values correspond to the ensemble mean.

**Table 2.** Uncertainty of maize projections of climatic indices (YEAR, annual impact) and stress indices (GRAIN and FLO for effective impact during grain filling and flowering, respectively) for the current climate (C) and the future scenario (A2), measured by the degree of coincidence among projections of each regional climate model (RCM)–scenario–location combination. Uncertainty is shown for events with 1 day (35-1d) and 5 consecutive days (35-5d) over the threshold of 35 °C. Average degree of coincidence across locations.

| Degree of coincidence of index 35-1d (%) | | | | | | |
|---|---|---|---|---|---|---|
| Location | YEAR C | YEAR A2 | GRAIN C | GRAIN A2 | FLO C | FLO A2 |
| NW-COAST | 77.8 | 57.8 | 100.0 | 57.8 | 100.0 | 77.8 |
| NW-INLAND | 77.8 | 42.2 | 80.0 | 46.7 | 91.1 | 62.2 |
| NE | 35.6 | 31.1 | 51.1 | 40.0 | 57.8 | 55.6 |
| N-PLATEAU | 53.3 | 48.9 | 53.3 | 64.4 | 55.6 | 84.4 |
| NE-VALLEY | 31.1 | 35.6 | 35.6 | 60.0 | 42.2 | 68.9 |
| CENTRE | 37.8 | 44.4 | 37.8 | 91.1 | 62.2 | 88.9 |
| S-PLATEAU 1 | 44.4 | 53.3 | 48.9 | 95.6 | 77.8 | 93.3 |
| S-PLATEAU 2 | 31.1 | 33.3 | 33.3 | 60.0 | 60.0 | 60.0 |
| SW-INLAND | 33.3 | 51.1 | 46.7 | 93.3 | 77.8 | 100.0 |
| SE-COAST | 51.1 | 66.7 | 64.4 | 77.8 | 73.3 | 82.2 |
| S-VALLEY | 33.3 | 53.3 | 55.6 | 86.7 | 68.9 | 82.2 |
| Mean | 45.0 | 47.6 | 55.0 | 71.7 | 69.4 | 78.1 |
| Degree of coincidence of index 35-5d (%) | | | | | | |
| Location | YEAR C | YEAR A2 | GRAIN C | GRAIN A2 | FLO C | FLO A2 |
| NW-COAST | 100.0 | 75.6 | – | 84.4 | – | 95.6 |
| NW-INLAND | 100.0 | 51.1 | 100.0 | 57.8 | 100.0 | 86.7 |
| NE | 84.4 | 46.7 | 88.9 | 60.0 | 100.0 | 86.7 |
| N-PLATEAU | 100.0 | 64.4 | 100.0 | 86.7 | 100.0 | 100.0 |
| NE-VALLEY | 64.4 | 60.0 | 64.4 | 97.8 | 73.3 | 100.0 |
| CENTRE | 48.9 | 97.8 | 57.8 | 88.9 | 75.6 | 95.6 |
| S-PLATEAU 1 | 51.1 | 100.0 | 68.9 | 100.0 | 100.0 | 100.0 |
| S-PLATEAU 2 | 60.0 | 80.0 | 62.2 | 93.3 | 100.0 | 95.6 |
| SW-INLAND | 44.4 | 100.0 | 68.9 | 97.8 | 86.7 | 98.9 |
| SE-COAST | 84.4 | 82.2 | 95.6 | 97.8 | 100.0 | 100.0 |
| S-VALLEY | 60.0 | 93.3 | 93.3 | 100.0 | 97.8 | 100.0 |
| Mean | 71.5 | 78.7 | 81.0 | 88.7 | 93.7 | 96.6 |

(–) No data means coincidence of ensemble members in projecting absence of events.

chosen in the A2 simulations are the same as in current climate (adaptations are not included); (2) crop growth duration in A2 presents a gradient of decrease from north to south and from coast to inland. A comparison between crop growth duration, flowering and maturity dates for two of the locations studied is presented in Fig. 7 for a northern location, NE, and a southern one, SW-INLAND. In the south, shortening of grain filling period is smaller than in the north because this phase begins 1.5 months earlier in the south (Fig. 7), although duration of this phenophase remains shorter in the south in A2 (Fig. 7). Consequently, computation of events during grain filling in A2 diminishes more in the south than in the north, while the number of events in A2 remains larger for south than for the north (compare SW-INLAND with NE lines in Fig. 5, for A2). This greater number of extreme events in south is coherent with the biggest projected maize yield decrease in southern Spain (Ruiz-Ramos and Mínguez, 2010).

It is underlined here that although the computation period for flowering (FLO index) is one month, this is a floating month that changes each year following evolution of thermal time. The corresponding effective impact shows that earlier flowering in A2 occurs in cooler periods in central and southern areas, thus reducing the risk of extreme $T_{max}$ events, while in the north flowering does not seem to escape $T_{max}$ extreme events. Simulations with different varieties and sowing dates should be chosen taking into account the effective impacts found here, and re-calculation of these indices could help to optimise this choice.

Consequently, projections for the IP show that extreme $T_{max}$ events may be a threat for summer crops, in particular during grain filling. These results are in line with those of Rosenweizg et al. (2000) in the USA, where decreases in agricultural yields were shown to be due to a combination of an increase in average temperatures, shortening crop duration, and an increase in extreme events. Results are also

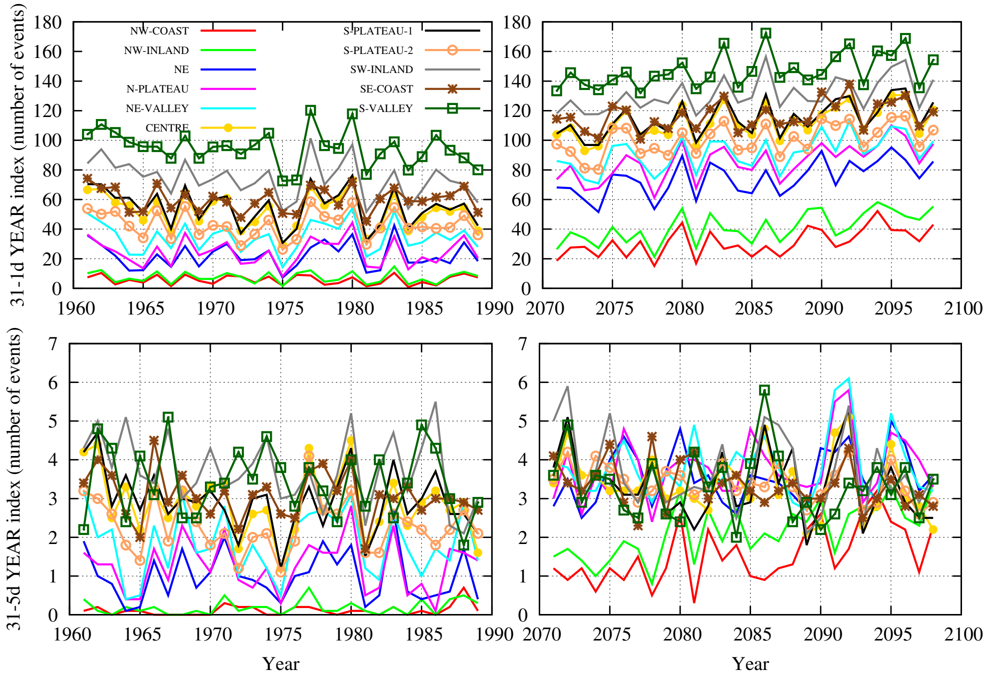


**Fig. 4.** Time series of extreme $T_{max}$ climatic indices (YEAR, annual impact from October to September) for irrigated spring wheat at locations of Fig. 1. Left column shows results for the current climate and right column for the future scenario A2. Upper plots show the number of events with 1 day over the threshold of 31 °C (31-1d), and below, the number of events with 5 consecutive days over 31 °C (31-5d) are shown. Values correspond to the ensemble mean.

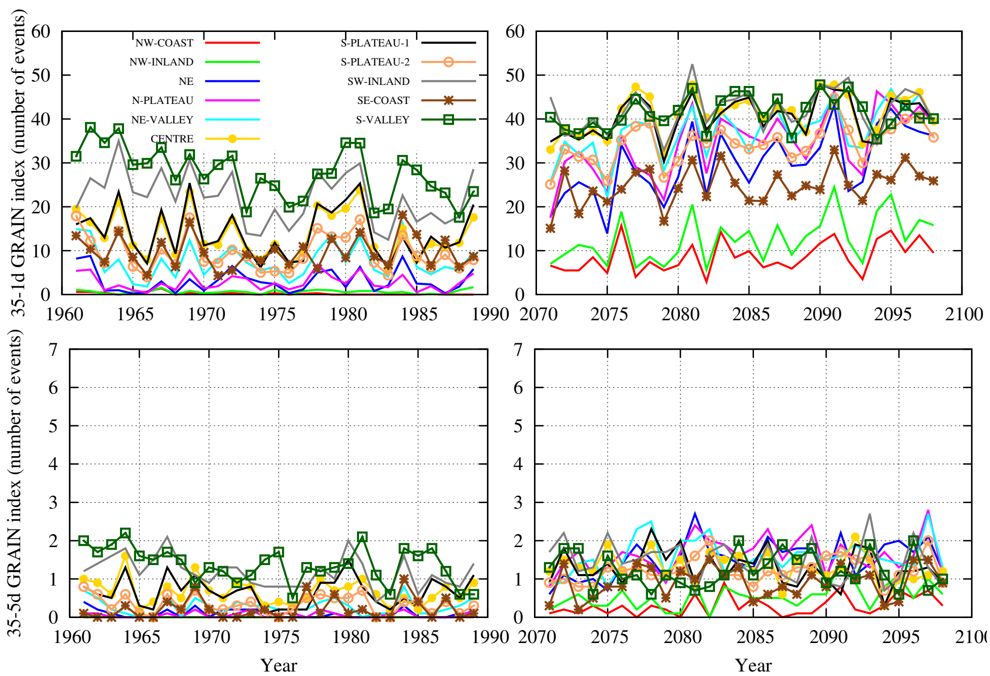


**Fig. 5.** Time series of extreme $T_{max}$ stress indices of effective impact during grain filling (GRAIN) for maize at locations of Fig. 1. Left column shows results for the current climate and right column for the future scenario A2. Upper plots show the number of events with 1 day over the threshold of 35 °C (35-1d), and below, the number of events with 5 consecutive days over 35 °C (35-5d) are shown. Values correspond to the ensemble mean.

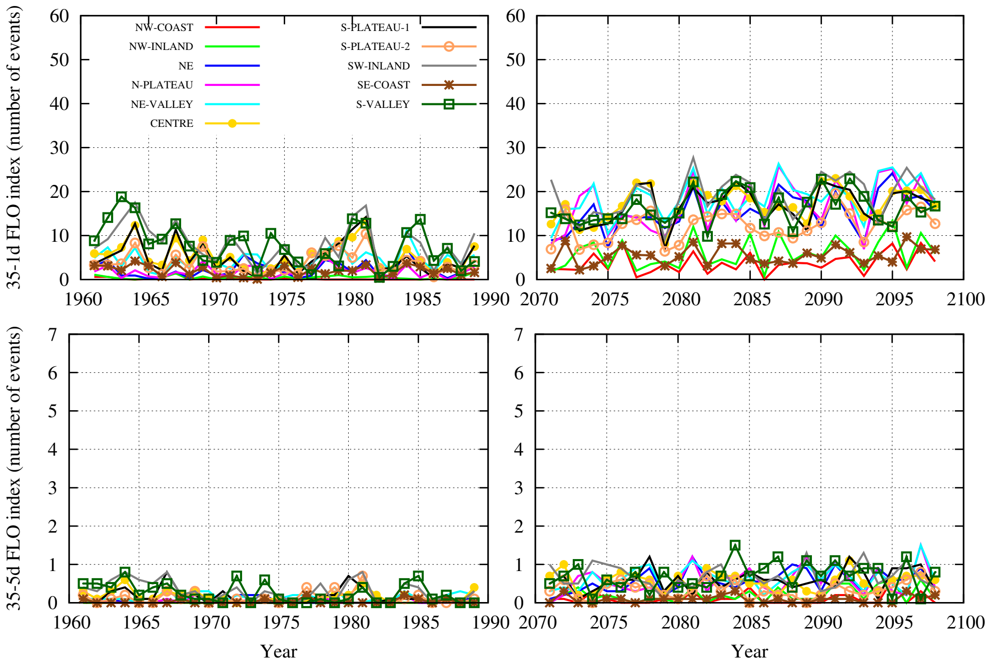


**Fig. 6.** Time series of extreme $T_{max}$ stress indices of effective impact during flowering (FLO) for maize at locations of Fig. 1. Left column shows results for the current climate and right column for the future scenario A2. Upper plots show the number of events with 1 day over the threshold of 35 °C (35-1d), and below, the number of events with 5 consecutive days over 35 °C (35-5d) are shown. Values correspond to the ensemble mean.

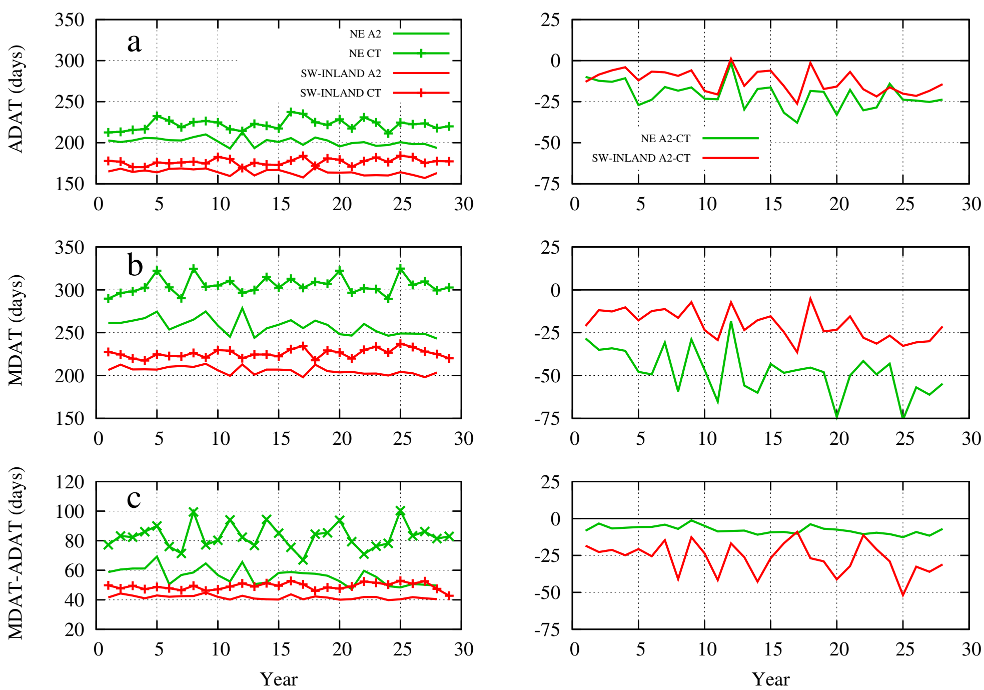


**Fig. 7.** Comparison of maize results between SW-INLAND and NE locations. Plots show time series of current climate (CT) and future projections (A2) on the the left, and variation between A2 scenario and current climate, calculated as A2-CT, on the right, for: flowering date in days **(a)**, physiological maturity date or end of crop cycle, in days **(b)**, and grain filling duration in days **(c)**.

**Table 3a.** Uncertainty of irrigated spring wheat projections of climatic indices (YEAR, annual impact) and stress indices (FLO, for effective impact during flowering) for the current climate (C) and the future scenario (A2), measured by the degree of coincidence among projections of each regional climate model (RCM)–scenario–location combination. Uncertainty is shown for events with 1 day (31-1d) and 5 consecutive days (31-5d) over the threshold of 31 °C. Average degree of coincidence across locations.

| | Degree of coincidence of index 31-1d (%) | | | |
|---|---|---|---|---|
| Location | YEAR C | YEAR A2 | FLO C | FLO A2 |
| NW-COAST | 64.4 | 60.0 | 100.0 | 100.0 |
| NW-INLAND | 40.0 | 46.7 | 100.0 | 100.0 |
| NE | 40.0 | 46.7 | 80.0 | 80.0 |
| N-PLATEAU | 44.4 | 68.9 | 100.0 | 100.0 |
| NE-VALLEY | 35.6 | 64.4 | 82.2 | 84.4 |
| CENTRE | 46.7 | 100.0 | 93.3 | 100.0 |
| S-PLATEAU 1 | 60.0 | 100.0 | 100.0 | 100.0 |
| S-PLATEAU 2 | 33.3 | 73.3 | 100.0 | 100.0 |
| SW-INLAND | 62.2 | 100.0 | 100.0 | 100.0 |
| SE-COAST | 53.3 | 100.0 | 100.0 | 100.0 |
| S-VALLEY | 68.9 | 100.0 | 100.0 | 100.0 |
| Mean | 51.4 | 80.0 | 96.2 | 97.0 |
| | Degree of coincidence of index 31-5d (%) | | | |
| Location | YEAR C | YEAR A2 | FLO C | FLO A2 |
| NW-COAST | 100.0 | 77.8 | – | – |
| NW-INLAND | 86.7 | 48.9 | – | – |
| NE | 57.8 | 80.0 | 100.0 | 100.0 |
| N-PLATEAU | 53.3 | 100.0 | 100.0 | – |
| NE-VALLEY | 46.7 | 100.0 | 100.0 | – |
| CENTRE | 75.6 | 100.0 | 100.0 | 100.0 |
| S-PLATEAU 1 | 77.8 | 95.6 | – | – |
| S-PLATEAU 2 | 51.1 | 95.6 | 100.0 | – |
| SW-INLAND | 95.6 | 91.1 | 100.0 | – |
| SE-COAST | 77.8 | 95.6 | – | – |
| S-VALLEY | 88.9 | 97.8 | – | – |
| Mean | 75.0 | 90.0 | 100.0 | 100.0 |

(–) No data means coincidence of ensemble members in projecting absence of events.

**Table 3b.** Uncertainty of irrigated spring wheat projections of climatic indices (YEAR, annual impact) and stress indices (GRAIN, for effective impact during grain filling) for the current climate (C) and the future scenario (A2), measured by the degree of coincidence among projections of each regional climate model (RCM)–scenario–location combination. Uncertainty is shown for events with 1 day (35-1d) and 5 consecutive days (35-5d) over the threshold of 35 °C. Average degree of coincidence across locations.

| | Degree of coincidence of index 35-1d (%) | | | |
|---|---|---|---|---|
| Location | YEAR C | YEAR A2 | GRAIN C | GRAIN A2 |
| NW-COAST | 75.6 | 55.6 | 100.0 | 100.0 |
| NW-INLAND | 71.1 | 46.7 | 100.0 | 100.0 |
| NE | 40.0 | 37.8 | 71.1 | 80.0 |
| N-PLATEAU | 48.9 | 57.8 | 82.2 | 84.4 |
| NE-VALLEY | 33.3 | 48.9 | 68.9 | 68.9 |
| CENTRE | 40.0 | 82.2 | 75.6 | 86.7 |
| S-PLATEAU 1 | 48.9 | 66.7 | 100.0 | 82.2 |
| S-PLATEAU 2 | 31.1 | 53.3 | 100.0 | 100.0 |
| SW-INLAND | 44.4 | 93.3 | 100.0 | 100.0 |
| SE-COAST | 53.3 | 86.7 | 100.0 | 100.0 |
| S-VALLEY | 42.2 | 91.1 | 100.0 | 100.0 |
| Mean | 47.5 | 67.6 | 91.4 | 91.8 |
| | Degree of coincidence of index 35-5d (%) | | | |
| Location | YEAR C | YEAR A2 | GRAIN C | GRAIN A2 |
| NW-COAST | 100.0 | 77.8 | 100.0 | – |
| NW-INLAND | 100.0 | 51.1 | – | – |
| NE | 82.2 | 53.3 | 100.0 | 100.0 |
| N-PLATEAU | 100.0 | 66.7 | 100.0 | – |
| NE-VALLEY | 64.4 | 71.1 | 100.0 | 100.0 |
| CENTRE | 55.6 | 100.0 | 100.0 | 100.0 |
| S-PLATEAU 1 | 53.3 | 100.0 | – | – |
| S-PLATEAU 2 | 60.0 | 80.0 | – | – |
| SW-INLAND | 53.3 | 100.0 | – | – |
| SE-COAST | 84.4 | 93.3 | – | – |
| S-VALLEY | 71.1 | 97.8 | – | – |
| Mean | 74.6 | 82.4 | 100.0 | 100.0 |

(–) No data means coincidence of ensemble members in projecting absence of events.

in agreement with the studies by Alcamo et al. (2007) and Moriondo et al. (2010a) for summer crops in the Mediterranean area (Spain, France, Italy and Greece), where increases in the frequency of extreme climate events during specific crop development stages were discussed to likely reduce the yield of summer crops.

### 3.2.2 Winter crops: spring wheat

Stress index estimated for grain filling (Fig. 8) and flowering (Fig. 9) periods is practically maintained in A2 in comparison with present climate results, with slight increment in 1d-type events and decrease in 5d-type. Therefore, results for annual impacts in future period significantly differ from those of effective impacts over the vulnerable periods, which are much smaller.

Uncertainties related to 31 °C stress indices (Table 3a, b) are in general smaller than those related to a 35 °C, because all RCMs project an increase of $T_{max}$ and the discrepancies are on the upper limits of the increase. Uncertainties in current climate are larger than in A2. Impact projections for vulnerable periods present very small uncertainty (mean coincidence above 90 %) when compared to annual impacts, and only locations in the northern plateau presented coincidence below 100 %. Uncertainties for 1d stress indices are larger than for 5d, the latter showing 100 % coincidence for vulnerable periods.

Yield impact projections in spring wheat have been shown to be subjected to very large uncertainties, even in the sign of the impact – i.e. yield increase or decrease – differing to those found in maize (Ruiz-Ramos and Mínguez, 2010). The

**Table 4.** Proportion of stress to climatic indices for maize, expressed as the percentage of effective impacts on grain filling and flowering with regard to annual impacts (GRAIN/YEAR and FLO/YEAR, respectively). Percentages are shown for the ensemble mean of current climate (C) and the future scenario (A2) of each location, for events with 1 day (35-1d) and 5 consecutive days (35-5d) over the threshold of 35 °C. Average percentage across locations.

| Relative index 35-1d (stress/climatic, %) | | | | |
|---|---|---|---|---|
| Location | GRAIN/YEAR C | GRAIN/YEAR A2 | FLO/YEAR C | FLO/YEAR A2 |
| NW-COAST | 68.4 | 77.1 | 48.2 | 33.7 |
| NW-INLAND | 63.9 | 79.9 | 49.0 | 39.4 |
| NE | 55.4 | 78.7 | 46.2 | 43.5 |
| N-PLATEAU | 82.9 | 78.8 | 57.3 | 39.4 |
| NE-VALLEY | 81.2 | 72.1 | 55.4 | 36.4 |
| CENTRE | 90.2 | 56.8 | 34.0 | 22.8 |
| S-PLATEAU 1 | 86.6 | 54.0 | 32.6 | 21.4 |
| S-PLATEAU 2 | 90.1 | 61.6 | 35.9 | 20.3 |
| SW-INLAND | 72.6 | 46.1 | 24.1 | 20.3 |
| SE-COAST | 69.9 | 38.6 | 13.1 | 8.1 |
| S-VALLEY | 58.6 | 37.7 | 15.5 | 14.6 |
| Mean | 73.2 | 59.9 | 35.5 | 26.2 |
| Relative index 35-5d (stress/climatic, %) | | | | |
| Location | GRAIN/YEAR C | GRAIN/YEAR A2 | FLO/YEAR C | FLO/YEAR A2 |
| NW-COAST | 3.3 | 76.7 | 3.3 | 24.8 |
| NW-INLAND | 15.0 | 67.4 | 15.0 | 24.8 |
| NE | 40.4 | 80.6 | 24.8 | 30.6 |
| N-PLATEAU | 82.9 | 78.8 | 57.3 | 39.4 |
| NE-VALLEY | 47.9 | 67.8 | 26.3 | 26.0 |
| CENTRE | 87.1 | 40.5 | 18.7 | 16.3 |
| S-PLATEAU 1 | 84.4 | 37.9 | 27.1 | 16.3 |
| S-PLATEAU 2 | 60.7 | 47.6 | 26.2 | 12.1 |
| SW-INLAND | 63.8 | 34.8 | 15.5 | 16.2 |
| SE-COAST | 45.9 | 27.1 | 3.6 | 2.3 |
| S-VALLEY | 49.9 | 33.0 | 7.9 | 19.5 |
| Mean | 48.2 | 52.0 | 16.8 | 19.5 |

small uncertainty found in the stress indices indicates that $T_{\max}$ events and temperatures do not play a significant role in the value of uncertainties, as occurred in maize in the northern and coastal areas.

Under current climate conditions, FLO/YEAR and GRAIN/YEAR ratios related to 1d events during grain filling reach 10 % maximum (Table 5). In A2, these ratios are reduced to a maximum of 2 %. Considering these values together with those of stress indices, projections of extreme events related to $T_{\max}$ do not seem to be harmful for winter crops in IP. This conclusion is in accord with that of Moriondo et al. (2010a), where heat stress in climate change scenarios CC was considered of minor importance in winter crops (winter wheat and sunflower) in the Mediterranean.

The majority of events in A2 are found inland in the northern third part of IP, which is indicative that in these regions $T_{\max}$ is greater during flowering to maturity. Figure 10 shows a comparison between variation in crop duration and flowering and maturity dates in two of the location studied, one in the north (NE) and another in the south (SW-INLAND). Grain filling in A2 is advanced ca. 1–1.5 months and occurs then in a cooler period in the south than in the north. This effect is similar to that in maize but less pronounced as grain filling duration is not so much shortened. This coincides with Mínguez et al. (2007), where yields of irrigated spring wheat not always decreased in A2 as opposed to maize. These differences with maize responses can be explained because projections of temperature increase are smaller during the seasons when wheat grows (autumn, winter and spring) than during summer (Christensen and Christensen et al., 2007).

### 3.3 General discussion

The climatic projections of extreme events evaluated in this work for IP are not translated homogenously into impact simulations; the analyses undertaken identify two driving

**Table 5.** Proportion of stress to climatic indices for irrigated spring wheat, expressed as the percentage of effective impacts on grain filling and flowering with regard to annual impacts (GRAIN/YEAR and FLO/YEAR, respectively). Percentages are shown for the ensemble mean of current climate (C) and the future scenario (A2) of each location, for events with 1 day and 5 consecutive days over the thresholds of 35 °C (35-1d, 35-5d) and 31 °C (31-1d, 31-5d). Average percentage across locations.

| Relative index 31-1d and 35-1d (stress/climatic, %) | | | | |
|---|---|---|---|---|
| | GRAIN/YEAR C | GRAIN/YEAR A2 | FLO/YEAR C | FLO/YEAR A2 |
| NW-COAST | 1.7 | 0.2 | 0.1 | – |
| NW-INLAND | 2.4 | 0.8 | 0.8 | 0.1 |
| NE | 7.5 | 1.0 | 1.4 | 0.2 |
| N-PLATEAU | 4.4 | 0.9 | 1.2 | 0.2 |
| NE-VALLEY | 9.2 | 1.5 | 1.7 | 0.4 |
| CENTRE | 5.8 | 0.9 | 0.6 | 0.2 |
| S-PLATEAU 1 | 3.4 | 0.3 | 0.2 | 0.1 |
| S-PLATEAU 2 | 1.4 | 0.2 | 0.1 | 0.1 |
| SW-INLAND | 0.2 | – | 0.1 | – |
| SE-COAST | 0.3 | 0.1 | 0.1 | – |
| S-VALLEY | 0.1 | 0.1 | – | 0.1 |
| Mean | 3.0 | 0.5 | 0.5 | 0.1 |
| Relative index 31-5d and 35-5d (stress/climatic, %) | | | | |
| | GRAIN/YEAR C | GRAIN/YEAR A2 | FLO/YEAR C | FLO/YEAR A2 |
| NW-COAST | 3.3 | – | – | – |
| NW-INLAND | – | – | – | – |
| NE | 1.3 | 0.1 | 0.4 | 0.1 |
| N-PLATEAU | 0.7 | – | 0.1 | – |
| NE-VALLEY | 2.2 | 0.5 | 1.3 | – |
| CENTRE | 2.0 | 0.3 | 0.3 | 0.1 |
| S-PLATEAU 1 | – | – | – | – |
| S-PLATEAU 2 | – | – | 0.1 | – |
| SW-INLAND | – | – | 0.1 | – |
| SE-COAST | – | – | – | – |
| S-VALLEY | – | – | – | – |
| Mean | 0.8 | 0.1 | 0.2 | – |

(–) No data means absence of events.

factors for impacts: cropping season and latitude. The different responses to climate change in maize and wheat show how cropping season determines impact. Furthermore, the results confirm the different capacity of crops and geographical regions to cope with climate change and extreme events, in agreement with Moriondo et al. (2010b). This capacity is independent of adaptations such as changes in sowing dates or cultivars. Earlier flowering occurs in both winter and summer crops but is more significant in the latter. Murphy (2000) and Christensen and Christensen (2007) showed that the largest increase of temperature in Europe is projected to be in the IP summer. Therefore, the increase of extreme events in general and in particular during summer is expected, with a greater impact on summer crops. Nevertheless, this study highlights that agronomic management and cultivars with a crop growth duration and/or with a different phenology adapted to the new climatic conditions can reduce effective impact. Crop insurance is also a tool for adaptation for dealing with increasing climate variability projected in future and information on the pattern of extreme events is needed.

In relation to the latitude factor, projections of effective impacts on crops by the end of C21 differ between the north and south of the IP, mainly due to an advanced flowering in the south. This spatial difference and its causes are similar to those found by Semenov and Stratonovitch (2010) who saw an analogous effect when comparing wheat responses in northern Europe (UK, also in Semenov (2009) and Mediterranean regions (Southern Spain, Central France and Central Italy). In these projections, a smaller relative increase in the probability of heat stress around flowering was found for southern locations because flowering was much earlier in southern parts of Europe.

Uncertainties associated to stress indices were medium to small, and smaller than uncertainty associated to YEAR indices. This can be explained because the computation

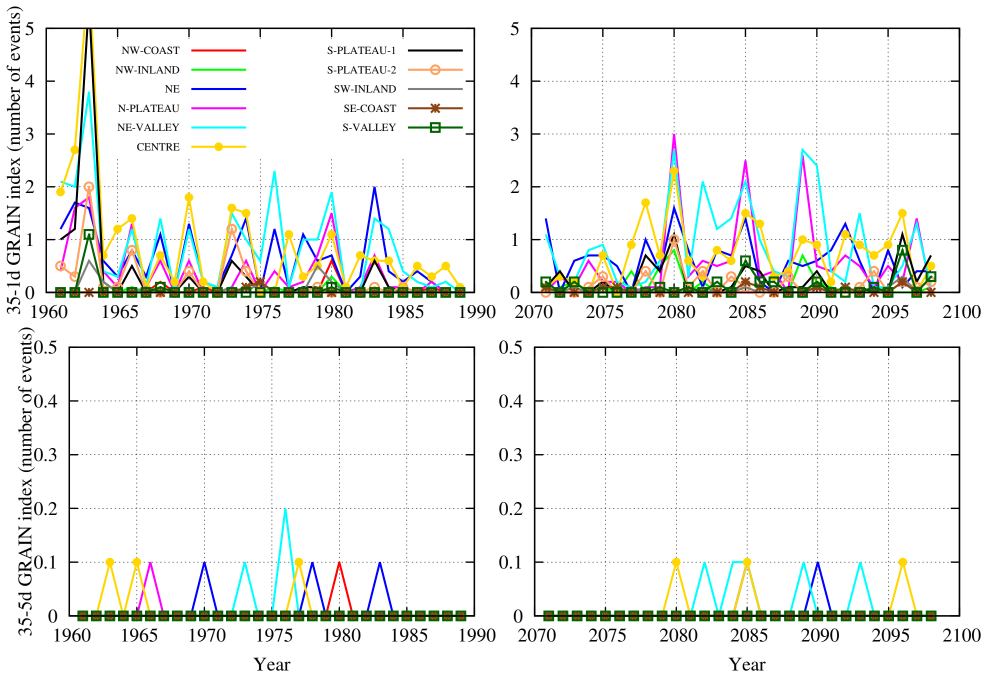


**Fig. 8.** Time series of extreme $T_{max}$ stress indices of effective impact during grain filling (GRAIN) for irrigated spring wheat at locations of Fig. 1. Left column shows results for the current climate and right column for the future scenario A2. Upper plots show the number of events with 1 day over the threshold of 35 °C (35-1d), and below, the number of events with 5 consecutive days over 35 °C (35-5d) are shown. Values correspond to the ensemble mean.

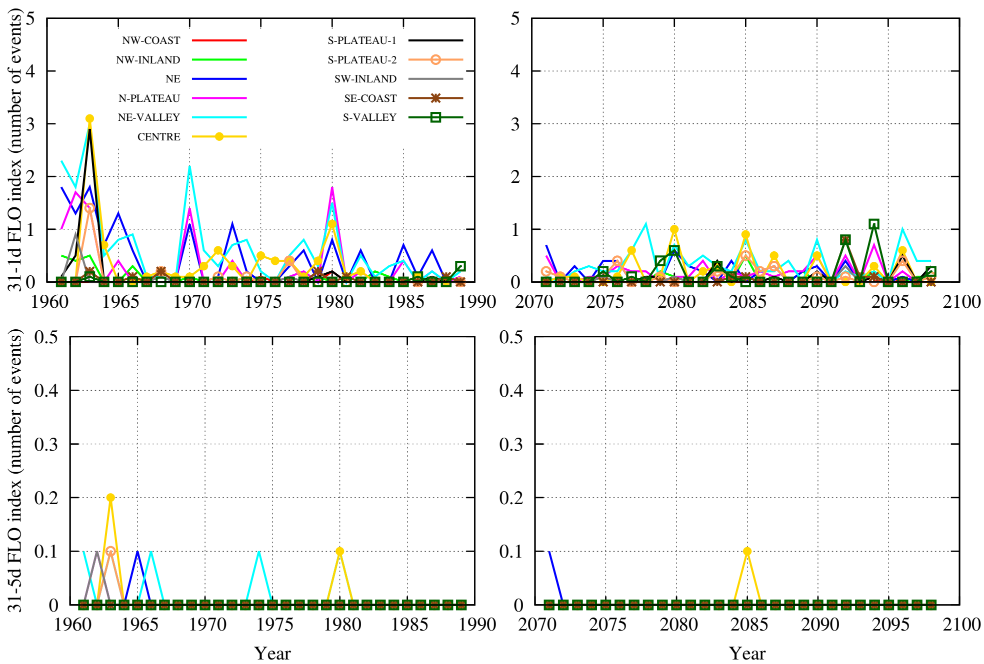


**Fig. 9.** Time series of extreme $T_{max}$ stress indices of effective impact during flowering (FLO) for irrigated spring wheat at locations of Fig. 1. Left column shows results for the current climate and right column for the future scenario A2. Upper plots show the number of events with 1 day over the threshold of 31 °C (31-1d), and below, the number of events with 5 consecutive days over 31 °C (31-5d) are shown. Values correspond to the ensemble mean.

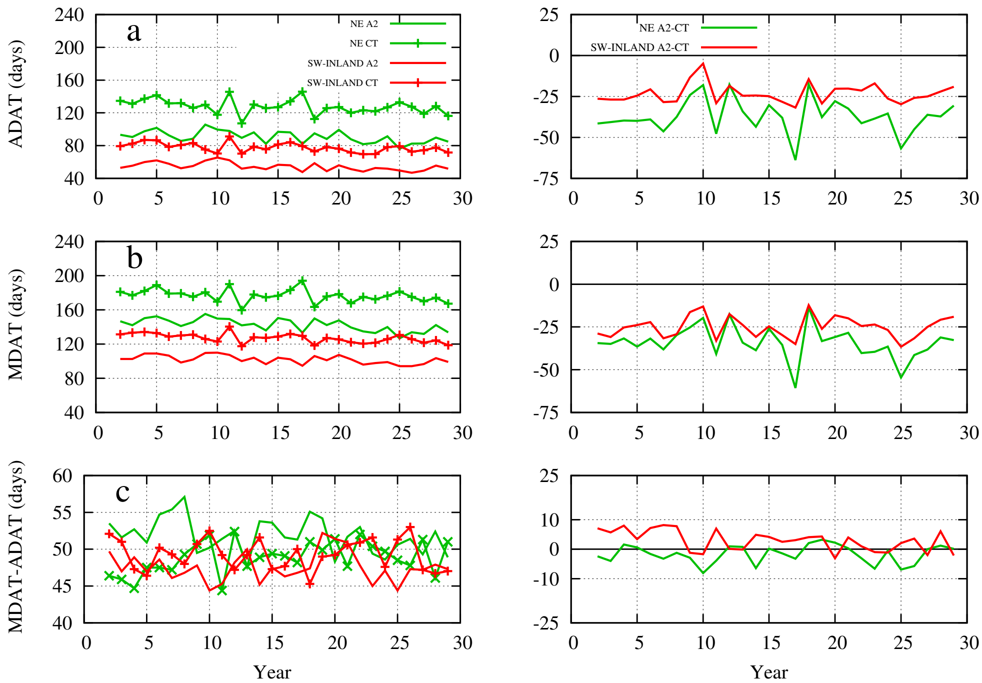


**Fig. 10.** Comparison of spring wheat results between SW-INLAND and NE locations. Plots show time series of current climate (CT) and future projections (A2) on the left, and variation between A2 scenario and current climate, calculated as A2-CT, on the right, for: flowering date in days **(a)**, physiological maturity date or end of crop cycle, in days **(b)**, and grain filling duration in days **(c)**.

period is shorter for stress indices. In addition, for maize those indices consider part or most of the summer (period of low uncertainty), and in wheat there are few events at the time of the vulnerable periods. Smaller uncertainties in A2 may be due to the small uncertainty in temperature projections (Sánchez and Míguez-Macho, 2010), which determine average temperature determining the changes in phenophase projections. However, uncertainties may be underestimated under current and future conditions because of a poor response of crop models to weather extremes (Easterling et al., 2007). Besides, there are additional sources of uncertainties not considered here, such as the driving GCM. Two out of the ten RCMs were not forced by the same GCM, including noise in our results. Nevertheless, the high degree of coincidence implies a robust result. Other uncertainty sources would be the emissions scenarios, and other cropping simulation options in these agricultural systems (e.g. rainfed conditions). For example, Moriondo and Bindi (2006), when comparing results derived from one RCM, one GCM and statistical downscaling, proposed that impacts derived from using RCMs may be overestimated – although they did not include a comparison derived from an ensemble of climate models. Nevertheless, the use of an ensemble of RCMs improves results interpretation and helps identify the limits and opportunities of their application, even taking into account that estimation of uncertainties in our work does not include all uncertainty sources. Furthermore, interpretation does not only restrict itself to the extreme events analysed here, but highlights how uncertainties of other related projections can be explained. In the case of projections where uncertainties are still too large to use results, it is expected that application of the scenarios generated by the European Project ENSEMBLES will help us to reduce them in several aspects: generation of climate projections up to 2050 or 2100 with a 25 km of horizontal resolution, different driving GCMs, and the statistical expression of uncertainty of an ensemble of 14 RCMs.

Nevertheless, the physical mechanisms of climate change behind the results of these simulations for extreme events need further and deeper analysis. Several authors are evaluating the effect of the global temperature increase on the modification of the hydrological cycle. The observations that support this relationship are not yet enough to establish it clearly. Recent works have reinforced this hypothesis through the enhancement of the probability of extreme warm days and decreases the probability of extreme cold days, and the reduction of wet days and drier conditions in summer over the Mediterranean (Sánchez et al., 2004), or the increase in the dry spells length over the IP (Sánchez et al., 2011) or the hydroclimatic intensity (Giorgi et al., 2011).

## 4 Conclusions

Agricultural impact of extreme events related to maximum daily temperature ($T_{\max}$) will increase under conditions of climate change in the Iberian Peninsula. Impact projections were calculated from an ensemble of RCMs. Temperature thresholds during vulnerable periods of crop development were used to estimate stress indices or effective impacts. These events will represent a threat for summer crops, but will not occur in the case of winter crops, thus showing the different vulnerability of the two growing seasons. These results contribute to explaining the decrease of maize yield projected in other studies that did not focus on $T_{\max}$. It also points to the need of considering these events when designing maize adaptation strategies. The different responses between northern and southern parts of IP were hightligthed: the effective impact was greater in the south but the increase of extreme events was larger in the north. This difference was due to a much earlier flowering date in the south. Finally, this work contributes to clarifying the causes of large uncertainties in the projections of spring wheat in the whole IP, and of maize in northern and coastal areas. This was achieved by excluding uncertainty related to $T_{\max}$ and extreme events projections as main components of the inconsistency found among these projections. The physical mechanisms of climate change over extreme events behind these results are likely to be related to the intensification of the hydrological cycle due to increased global temperatures, although further research is needed to confirm these hypotheses.

*Acknowledgements.* This work was funded by the Comisión Interministerial de Ciencia y Tecnología (CICYT) Project AGL2008-00385/AGR and by the "Viceconsejería de Ciencia y Tecnología" of the "Junta de Castilla-La Mancha", Projects: PEII10-0248-5680 and POII10-0255-8836. We thank Esther Sánchez Herranz from AgSystems group for her work in managing the crop database and preparing the manuscript.

Edited by: A. Gobin
Reviewed by: two anonymous referees

## References

Ainsworth, E. A., Leakey, A. D. B.,Bernacchi, J. C., Rogers, A, Stephen, P. L., and Ort, D. R.: Elevated $CO_2$ effects on plant carbon, nitrogen, and water relations: six important lessons from FACE, J. Exp. Botany., 60, 2859–2876, 2009.

Alcamo, J., Moreno, J. M., Nováky, B., Bindi, M., Corobov, R., Devoy, R. J. N., Giannakopoulos, C., Martin, E., Olesen, J. E., and Shvidenko, A.: Europe, in: Climate Change 2007: Impacts, Adaptation and Vulnerability. Contribution of Working Group II to the Fourth Assessment Report of the Intergovernmental Panel on Climate Change, edited by: Parry, M. L., Canziani, O. F., Palutikof, J. P., van der Linden, P. J., and Hanson, C. E., Cambridge University Press, Cambridge, UK, 541–580, 2007.

Al-Khartib, K. and Paulsen, G. M.: Mode of high temperature injury to wheat during grain development, Plant. Physiol., 61, 363–368, 1984.

Beniston, M., Stephenson, D. B., Christensen, O. B., Ferro, C. A. T., Frei, C., Goyette, S., Halsnaes, K., Holt, T., Jylhä, K., Koffi, B., Palutikof, J., Schöll, R., Semmler, T., and Woth, K.: Future extreme events in European climate: an exploration of regional climate model projections, Clim. Change, 81 (S1), 71–95, doi:10.1007/s10584-006-9226-z, 2007.

Christensen, J. H. and Christensen, O. B.: A summary of the PRUDENCE model projections of changes in European climate during this century, Clim. Change, 81 (S1), 7–30, 2007.

Christensen, J. H., Hewitson, B., Busuioc, A., Chen, A., Gao, X., Held, I., Jones, R., Kolli, R. K., Kwon, W-T., Laprise, R., Magaña Rueda, V., Mearns, L., Menéndez, C. G., Räisänen, J., Rinke, A., Sarr, A., and Whetton, P.: Regional Climate Projections, in: Climate Change 2007: The Physical Science Basis. Contribution of Working Group I to the Fourth Assessment Report of the Intergovernmental Panel on Climate Change, edited by: Solomon, S., Qin, D., Manning, M., Chen, Z., Marquis, M., Averyt, K. B., Tignor, M., and Miller, H. L. Cambridge University Press, Cambridge, United Kingdom and New York, NY, USA, 2007.

Ciais, P. H., Reichstein, M., Viovy1, N., Granier, A., Ogée, J., Allard, V., Aubinet, M., Buchmann, N., Bernhofer, C. H. R., Carrara, A., Chevallier, F., De Noblet, N., Friend, A. D., Friedlingstein, P., Grünwald, T., Heinesch, B., Keronen, P., Knohl, A., Krinner, G., Loustau, D., Manca, G., Matteucci1, G., Miglietta, F., Ourcival, J. M., Papale, D., Pilegaard, K., Rambal, S., Seufert, G., Soussana, J. F., Sanz, M. J., Schulze, E. D., Vesala, T., and Valentín, R. Nature, 437, 529–533, doi:10.1038/nature03972, 2005.

Coehlo, D. T., and Dale, R. F.: An energy-crop growth variable and temperature function for predicting corn growth and development: Planting to silking, Agron. J., 72, 503–510, 1980.

Del Río, S., Fraile, R., Herrero, L., and Penas, A.: Analysis of recent trends in mean maximum and minimum temperatures in a region of the NW of Spain (Castilla y León). Theor. Appl. Climatol., 90, 1–12, doi:10.1007/s00704-006-0278-9, 2007.

Dequé, M., Rowell, D. P., Lüthi, D., Giorgi, F., Christensen, J. H., Rockel, B., Jacob, D., Kjellström, E., Castro, M., and Van den Hurk, B.: An intercomparison of regional climate simulations for Europe: assessing uncertainties in model projections, Climate Change 81 (S1), 53–70, 2007.

Diffenbaugh, N. S., Pal, J. S., Giorgi, F., and Gao, X.: Heat stress intensification in the Mediterranean climate change hotspot, Geophys. Res. Lett., 34, L11706, doi:10.1029/2007GL030000, 2007.

Easterling, W. E., Aggarwal, P. K., Batima, P., Brander, K. M., Erda, L., Howden, S. M., Kirilenko, A., Morton, J., Soussana, J.-F., Schmidhuber, J., and Tubiello, F. N.: Food, fibre and forest products, in: Climate change 2007: impacts, adaptation and vulnerability. Contribution of Working Group II to the Fourth Assessment Report of the IPCC, edited by: Parry, M. L., Canziani, O. F., Palutikof, J. P., van der Linden, P. J., and Hanson, C. E., Cambridge University Press, Cambridge, 273–313, 2007.

Field, A.: Discovering statistics using SPSS (2nd edn) Sage Publications, London, 2005.

Gardner, F. P., Pearce, R. B., and Mitchell, R. L.: Physiology of Crop Plants, Iowa State University Press, Ames., 327 pp., 1985.

Gilmore, E. C., and Rogers, J. S.: Heat units as a method of measuring maturity in corn, Agron. J., 50, 611-615, 1958.

Giorgi, F., Hewitson, B., Christensen, J., Hulme, M., Von Storch, H., Whetton, R., Jones, R, Mearns, L. O. and Fu, C.: Regional climate information: evaluations and projections, in: Climate change 2001: the scientific basis, Contribution of Working Group I to the Third Assessment Report of IPCC, edited by: Houghton, J. T., Ding, Y., Griggs, D. J., Noguer, M., van der Linden, P. J., Dai, X., Maskell, K., and Johnson, C. A., Cambridge University Press, Cambridge, 739–768, 2001.

Giorgi, F., Im, E. S., Coppola, E., Diffenbaugh, N. S., Gao, X. J., Mariotti, L., and Shi, Y.: Higher Hydroclimatic Intensity with Global Warming, J. Climate, 24, 5309–5324, doi:10.1175/2011JCLI3979.1, 2011.

Guereña, A., Ruiz-Ramos, M., Diaz-Ambrona, C.H., Conde, J.R., and Mínguez, M.I.: Assessment of climate change and agriculture in Spain using climate models, Agron. J., 93, 237–249, 2001.

Hertig, E., Seubert, S., and Jacobeit, J.: Temperature extremes in the Mediterranean area: trends in the past and assessments for the future, Nat. Hazards Earth Syst. Sci., 10, 2039–2050, doi:10.5194/nhess-10-2039-2010, 2010.

Iglesias, A. and Mínguez, M. I.: Perspectives for maize production in Spain under climate change, in: Climate change and agriculture: analysis of potential international impacts, edited by: Rosenzweig, C., Allen, L. H. Jr, Harper, L. A., Hollinger, S. E., and Jones, J. W., Vol 13, American Society of Agronomy, Madison, WI., 259–273, 1995.

Jacob, D., Barring, L., Christensen, O. B., Christensen, J. H., de Castro, M., Dequé, M., Giorgi, F., Hagemann, S., Hirschi, M., Jones, R., Kjellström, E., Lenderink, G., Rockel, B., Snchez, E., Schär, C., Seneviratne, S. I., Somot, S., van Ulden A., and van den Hurk, B.: An inter-comparison of regional climate models for Europe: model performance in present-day climate, Clim. Change, 81(S1), 31–52, 2007.

Jones, C. A. and Kiniry, J. R.: CERES-Maize: A simulation model of maize growth and development, Texas A&M University Press, College Station, TX, 1986.

Kjellström, E., Bärring, L., Jacob, D., Jones, R., Lenderink, G., and Schär, C.: Modelling daily temperature extremes: recent climate and future changes over Europe, Clim. Change, 81 (S1), 249–265, doi:10.1007/s10584-006-9220-5, 2007.

Loomis, R. S. and Connor, D. J.: Crop ecology: productivity and management in agricultural systems, Reprint with corrections, Cambridge University Press, Cambridge, 1996.

López-Cedrón, F. X., Boote, K. J., Ruíz-Nogueira, B., and Sau, F.: Testing CERES-Maize versions to estimate maize production in a cool environment, Eur. J. Agron., 23, 89–102, 2005.

Mariscal, M. J.: Efectos de la fecha de siembra sobre el crecimiento, desarrollo, producción y uso de agua de genotipos de trigo que difieren en necesidades de vernalización, MSc thesis, Universidad de Córdoba, 1993.

Mearns, L. O., Katz R. W., and Schneider, S. H.: Extreme High-Temperature Events: Changes in Their Probabilities with Changes in Mean Temperature, J. Clim. Appl. Meteor., 23, 1601–1613, 1984.

Mearns, L. O., Giorgi, F., Mcdaniel, L., and Shields, C.: Climate scenarios for the southeast U.S. based on GCM and regional model simulations, Clim. Change, 60, 7–35, 2003.

Mínguez, M.I., Ruiz-Ramos, M., Díaz-Ambrona, C. H., and Quemada, M.: Productivity in agricultural systems under climate scenarios, Evaluation and adaptation, J. Phys., 121, 269–281, 2004.

Mínguez, M.I., Ruiz-Ramos, M., Díaz-Ambrona, C. H., Quemada, M., and Sau, F.: First-order impacts on winter and summer crops assessed with various high-resolution climate models in the Iberian Peninsula, Clim. Change, 81(SI), 343–355, 2007.

Moriondo, M., and Bindi, M.: Comparison of temperatures simulated by GCMs, RCMs and statistical downscaling: potential application in studies of future crop development, Clim. Res., 30, 149–160, 2006.

Moriondo, M., Giannakopoulos, C., and Bindi, M.: Climate change impact assessment: the role of climate extremes in crop yield simulation, Clim. Change, doi:10.1007/s10584-010-9871-0, 2010a.

Moriondo, M., Bindi, M., Kundzewicz, Z. W., Szwed, M., Chorynski, A., Matczak, P., Radziejewski, M., McEvoy, D., and Wreford, A.: Impact and adaptation opportunities for European agriculture in response to climatic change and variability, Mitig. Adapt. Strateg. Glob. Change., 15, 657–679, doi:10.1007/s11027-010-9219-0, 2010b.

Murphy, J.: Predictions of climate change over Europe using statistical and dynamical downscaling techniques, Int. J. Climatol., 20, 489–501, 2000.

Nakicenovic, N. and Swart, R.: Emissions scenarios. Special Report of the Intergovernmental Panel on Climate Change, Cambridge University Press, Cambridge,2000.

Porter, J. R. and Gawith, M.: Temperatures and the growth and development of wheat: a review. Eur. J. Agron., 10, 23–36, 1999.

Quemada, M., Cabrera, M. L., and McCracken, D. V.: Nitrogen released from surface-applied cover crop residues: evaluating CERES-N. Agron. J., 89, 723–729, 1997.

Rebollo, J.: Calibración y verificación de un modelo de simulación de trigo (Ceres-Wheat) para las condiciones del Valle del Guadalquivir y su aplicación al análisis de estrategias de riego. MSc thesis, Universidad de Córdoba, 1993.

Ritchie, J. T. and Otter, S.: Description and performance of CERES-Wheat: a user-oriented wheat yield model. In: Serv NTI (ed). ARS wheat yield project, Vol ARS-38. Springfield, MI, pp 159–175, 1985.

Rosenzweig, C., Iglesias, A., Yang, X. B., Epstein, P. R., and Chivian, E.: Climate Change and U.S. Agriculture: The Impacts of Warming and Extreme Weather Events on Productivity, Plant Diseases, and Pests. Center for health and the global enviroment, Boston, MA, 2000.

Ruiz-Ramos, M. and Mínguez, M. I.: Evaluating uncertainty in climate change impacts on crop productivity in the Iberian Peninsula, Clim. Res., 44, 69–82, 2010.

Sadras, V. O. and Monzón, J. P.: Modelled wheat phenology captures rising temperature trends: Shortened time to flowering and maturity in Australia and Argentina, F. Crop. Res., 99, 136–146, 2006.

Sánchez, E., Gallardo, C., Gaertner, M. A., Arribas, A., and Castro, M.: Future climate extreme events in the Mediterranean simulated by a regional climate model: a first approach. Glob. Planet Change, 44, 163-180, 2004.

Sánchez, E. and Miguez-Macho, G.: Regional Climate Projections over the Iberian Peninsula: Climate Change Scenarios Modeling. in: Climate in Spain: Past, Present and Future, edited by: Pérez, F. and Boscolo, R., Regional climate change assessment report,

Clivar Spain, 2010.
Sánchez, E., Domínguez, M., Romera R., López de la Franca, N., Gaertner, M. A., Gallardo, C., and Castro, M.: Regional modeling of dry spells over the Iberian Peninsula for present climate and climate change conditions, Clim. Change 107, 625–634, doi:10.1007/s10584-011-0114-9, 2011.
Schär, C., Vidale, P.L., Lüthi, D., Frei, C., Häberli, C., Liniger, M.A., and Appenzeller, C.: The role of increasing temperature variability in European summer heatwaves, Nature, 427, 332–336, doi:10.1038/nature02300, 2004.
Semenov, M.: Impacts of climate change on wheat in England and Wales, J. R. Soc. Interface, 6, 343–350, doi:10.1098/rsif.2008.0285, 2009.
Semenov, M. and Stratonovitch, P.: Use of multi-model ensembles from global climate models for assessment of climate change impacts, Clim. Res., 41,1–14, doi:10.3354/cr00836, 2010.
Tsuji, G. Y., Uehara, G., and Balas, S.: DSSAT Version 3. University of Hawaii, Honolulu, HI, 1994.
Wheeler, T. R., Craufurd, P. Q., Ellis, R. H., Porter, J. R., and Vara Prasad, P. V.: Temperature variability and the yield of annual crops, Agr. Ecosyst. Environ., 82, 159–167, 2000.